Amoxicillin exposure significantly increases the population and virulence of antibiotic-resistant Klebsiella pathogen in the simulated human intestinal microbiota

Lei Liu
Nankai University
Zeyou Chen
Nankai University
Qing Wang
Hebei University of Engineering
Jingliang Shi
Nankai University
Wenjing Bi
Nankai University
Siyi Wang
Nankai University
Yanyu Gao
Nankai University
Huai Lin
Nankai University
Hongmei Qi
Nankai University
Siyuan Zhu
Nankai University
Jing Yang
Nankai University
Yingang Xue
Changzhou Environmental Monitoring Center
Daqing Mao
Nankai University
Yi Luo (luoy@nankai.edu.cn)
Nankai University https://orcid.org/0000-0002-6732-7935

Research

Keywords: Amoxicillin (AMX); Antibiotic resistance; Human disease-related pathways; Klebsiella; Simulator of the human intestinal microbial ecosystem (SHIME); Virulence.

Posted Date: January 22nd, 2020

DOI: https://doi.org/10.21203/rs.2.21625/v1

Abstract

Background: The extensive use and misuse of antibiotics have caused the emergence and spread of antibiotic resistance among bacterial pathogens, which is threatening to this idyllic world. The human intestinal microbiota is significant to health, while its composition and stability are easily perturbed by antibiotic exposure. However, the association between antibiotic exposure and the abnormal bloom of opportunistic pathogens in human gut, and its health implications are not fully understood. Therefore, this study investigated the influence of amoxicillin (AMX), one of the most prescribed antibiotics in human life, on human intestinal microbiota using the simulator of the human intestinal microbial ecosystem (SHIME). Results: Our results suggest that AMX exposure could cause the substantial effect on human intestinal microbiota in different colon regions, with most significant alteration in ascending colon. Intriguingly, AMX significantly increased the abundance of antibiotic-resistant Klebsiella pathogen in gut microbiota, resulting in the enrichment of human disease-related pathways. By isolation of Klebsiella strains from SHIME before and after exposure to AMX, we also observed that the virulence phenotypes of these pathogens including biofilm formation, serum resistance, and Galleria mellonella infection were significantly increased after AMX administration. The genotype analysis from whole genome sequencing indicated that the enhanced virulence phenotypes were plausibly caused by the mutations of virulence factors relevant to fimbriae, lipopolysaccharide, capsule, and siderophores. More importantly, the effects from AMX administration could not be fully recovered after two-week drug discontinuance, showing the potential long-term adverse influence of this antibiotic. Conclusions: This study for the first time demonstrates that AMX used for the treatment of bacterial infections may cause adverse effects on human health via significantly increasing population and virulence of intestinal Klebsiella opportunistic pathogen. Given that inherent resistance to β-lactam already poses a significant therapeutic challenge for Klebsiella infections, the AMX-induced virulence increasing phenomenon found in this study undoubtedly further increases its health risk.

Background

The human intestine constitutes an especially large and diverse microbial habitat that is colonized mainly by bacteria but also by archaea, viruses, and eukaryotes [1]. Previous studies have manifested that the human intestinal microbiota comprises about 150 times more genes than the human genome, making it become ‘another’ genome of human beings [2, 3]. Moreover, the human intestinal microbiota has been demonstrated to provide numerous important functions for human health including nutrient supply by fermentation of indigestible dietary polysaccharides, synthesis of essential amino acids and vitamins, modulating the immune function, protection from infection of pathogens, etc. [4, 5].

Antibiotic therapy has saved millions of human lives since its discovery in the 1940s, however indiscriminately killing or preventing the growth of both pathogenic and commensal bacteria is its major drawback. In recent years, the adverse influence of antibiotics on human health has become a public concern since it could cause the dysbiosis of human intestinal microbiota, resulting multiple human diseases [6, 7]. Otherwise, antibiotics may also promote the evolution, proliferation, and maintenance of

antibiotic resistant bacteria (ARB) and antibiotic resistance genes (ARGs) in the human gut [8, 9]. In general, both *in vivo* and *in vitro* experiments were widely used in examination of antibiotic influence on gut microbiota [10-15]. *In vivo* experiments would reflect the actual influences of antibiotics on human body, while the detected fecal samples are generally stood for the distal intestinal microbiota that could not reveal the impacts of antibiotics on different gut regions [16, 17]. Instead, *in vitro* simulator with different gut regions can reproduce human gut environment in the absence of host cells, thus allow to examine the effects of antibiotics on different regions of human intestinal microbiota without the disturbances of neurohumoral regulation, the individual differences, dietary habits, and physiological status. However, most classic *in vitro* models such as single-stage chemostats and semi-continuous fermenters could neither integrate the entire gastrointestinal tract nor maintain microbiome stability over an extended timeframe, and the results obtained generally need the confirmation of *in vivo* experiments [18]. As a widely used multi-compartment simulator, the simulator of the human intestinal microbial ecosystem (SHIME) has been used to study microbiota interactions in gut and the effects of toxic compounds on gut microbiota [19]. To date using SHIME model to study the influences of antibiotics on human gut microbiota is still rare.

Amoxicillin (AMX), an inexpensive but broad-spectrum oral penicillin-type β-lactam antibiotic, is one of the most prescribed medicine in human life. It kills bacteria by interfering with the synthesis of the bacterial cell wall peptidoglycan [20, 21]. Over the last several years, extensive studies have provided valuable insights into the effects of AMX on human intestinal microbiota [22-25]. However, the real impacts caused by AMX on human gut flora is still controversy. In addition, the association between AMX exposure and the abnormal bloom of opportunistic pathogens in human gut, and associated health implications are not fully understood. Therefore, this study investigates the influence of AMX on human intestinal microbiota in SHIME model. Considering the reasonable dosage of AMX for adult human study is about 750 to 1500 mg/day and only half volume of adult gut can be simulated in used SHIME model, 600 mg/day of AMX was used to examine its impacts on human gut microbiota and associated functional pathways [22, 24]. Moreover, we isolated *Klebsiella* strains from SHIME before and after exposure to AMX, and detected their virulence phenotypes including biofilm formation, serum resistance, and *Galleria mellonella* infection. Our data suggest that AMX exposure caused an adverse impact on the gut microbiota with significantly increased antibiotic-resistant *Klebsiella* and human disease-related pathways. Furthermore, exposure to AMX significantly increased the virulence of antibiotic-resistant *Klebsiella*, which may be attributed to the mutations of fimbriae, lipopolysaccharide, capsule, and siderophores virulence factors. To the best of our knowledge, this study for the first time demonstrates that AMX used for the treatment of bacterial infections may cause adverse effects on human health via significantly increased population and virulence of intestinal *Klebsiella* opportunistic pathogen.

Results

AMX exposure significantly increased *Klebsiella* abundance in simulated gut microbiota

To reveal the effects of AMX treatment on the gut bacterial community, AMX was administrated into SHIME model in Fig. 1A. Before the exposure, the system was initially operated in the absence of AMX for three weeks, then 600 mg/day of AMX was injected into the system for another week, followed by the last two weeks of operation after the drug discontinuance. Fecal samples at 14, 21, 24, 28, 35 and 42 days from the ascending, transverse and descending colon vessels were collected for 16S rRNA gene amplicon sequencing. Specifically, these samples represent samples before AMX exposure, after 600 mg/day of AMX treatment, and after termination of AMX (Fig. 1A). The bacteria compositions at the genus and phylum levels at different sampling points were shown in Fig. 1B and Fig. S1, respectively. In terms of the taxonomic assignment at the phylum level, *Bacteroidetes*, *Proteobacteria*, and *Firmicutes* were the three most dominant bacterial phyla in both ascending (accounting for total percent of 91.7%-98.0%) and transverse colon (77.5%-88.8%), while three most abundant phyla in the descending colon were *Proteobacteria*, *Bacteroidetes*, and *Synergistetes* (81.8%-91.1%) (Fig. S1). Regarding genus level, *Bacteroides*, *Klebsiella*, *Pseudomonas*, and *Pyramidobacter* were predominant in all three colon regions (Fig. 1B). Linear discriminant analysis effect size (LEfSe) results indicated that AMX exposure caused obvious decreases in *Bifidobacterium*, *Phascolarctobacterium* and *Parabacteroides* (Fig. 1C), in accompanying with significant increases in *Klebsiella* (opportunistic pathogen, LSD = 5.26) and *Bacteroides uniformis* (probiotics, LSD = 4.75). As *Klebsiella* genus is an important antibiotic-resistant pathogen in human gut and its unnormal bloom is often associated with multiple diseases, thus we put more attentions on the increased *Klebsiella* abundance in this study (Fig. 1D). Furthermore, the significant ($p < 0.05$) enrichment of *Klebsiella* was observed for both ascending (increased from 1.6% to 32.9%) and transverse colons (increased from 1.5% to 14.0%). Although the abundance of *Klebsiella* exhibited a partially reduction after the discontinuance of AMX for 2 weeks, the *Klebsiella* abundance was still obviously higher compared to AMX-free controls (Fig. 1D). For descending colon, a similar higher *Klebsiella* abundance was also observed although no statistically significant difference between AMX-exposed treatments and AMX-free controls.

Positive correlations between gene numbers of human disease-related pathways and the *Klebsiella* abundance

The functional composition of bacterial communities was predicted by PICRUST, gene numbers of human disease-related function pathways in bacterial communities in three regions of the colon at different sampling time were obtained in the heatmap (Fig. 2). The results suggested that with the time increased, gene numbers of human disease-related pathways including cancer, drug resistance, infectious diseases, metabolic diseases and neurosurgery diseases exhibited firstly increased then marginally decreased. Regardless of the colon region, AMX exposure significantly enhanced gene numbers of the above pathways, with the greatest enhancement effect in the ascending colon. For example, compared to C-A2 (AMX-free treatment sample) that collected from the ascending colon before AMX administration, gene numbers of the drug resistance pathways were 3.4-4.4 times enriched in the AMX-A2 (AMX exposed treatment sample) that collected after AMX administration for seven days. Similarly, gene numbers of other pathways including bladder cancer, African trypanosomiasis, pertussis and Alzheimer's disease were nearly 4-5.6 times enriched in the AMX-A2 sample than C-A2. Moreover, these human disease-related

pathway gene numbers were still maintained at relatively higher levels (about 1.7-2.4 times enriched than AMX-free controls) after the discontinuance of AMX for two weeks.

To explore the potential factors responsible for the changed gene numbers of human disease-related pathways during the incubation period, pearson correlation analyses were performed between gene numbers of pathways and the abundance of *Klebsiella*. As shown in Fig. 2, the pathway gene numbers of β-lactam resistance, cationic antimicrobial peptide (CAMP) resistance, and vancomycin resistance all had strong positive correlations with the abundances of *Klebsiella* (Correlation coefficient R was 0.973, 0.944, and 0.974, respectively; $p < 0.001$). Similarly, the correlations between gene numbers of other human disease-related pathways like cancer, infectious diseases, metabolic diseases, and neurosurgery diseases and the *Klebsiella* abundance were also positive. Especially the correlation coefficients of pathway gene numbers of bladder cancer, Chagas disease, type II diabetes mellitus, and Huntington's disease with *Klebsiella* abundance were 0.974, 0.980, 0.969, and 0.968 ($p < 0.001$), respectively.

Molecular mechanisms for *Klebsiella*'s contribution to human diseases

In order to further explore the potential molecular mechanisms for the contribution of *Klebsiella* to human diseases, we isolated *Klebsiella* strains from AMX-exposed sample AMX-A2 (the most significant effect on human diseases happened in this sample). Using a *Klebsiella*-specific culture medium, a total of 8 *Klebsiella* strains were isolated, within which NKU_KlebA1, NKU_KlebA2, NKU_KlebA4, and NKU_KlebA5 possessed all 5 detected ARGs related to drug resistance pathways (*bl2b_tem1* and *bl2be_shv2* related to β-lactam resistance; *arna* and *rosb* related to CAMP resistance; and *vang* related to vancomycin resistance) (Table S1). Considering NKU_KlebA1 from AMX-exposed treatment has a close genetic distance with the *Klebsiella* strains from AMX-free control in the 16S rRNA gene-based phylogenetic tree (Fig. 4D), this strain was chosen for further investigation of its whole-genome. The results demonstrated that *K. pneumoniae* NKU_KlebA1 possesses a ~ 5,250 kp chromosome containing about 5,880 protein-encoding genes with average lengths of 799 bp and average G+C content of 58.6%, as detailed in Table S2 and Fig. 3A. The mobile elements and metabolic systems of this strain were summarized in supplemental Excel S1. Mobile elements were exogenous genome fragments that help bacteria competing for ecological niche and survival in host, resulting in 20 genomic islands, 5 prophages and 4 clustered regularly interspaced palindromic repeats/CRISPR-associated proteins (CRISPR/Cas) systems found in NKU_KlebA1. Meanwhile, metabolic systems of this strain consists of 3 secondary metabolites synthesize gene clusters and 6 carbohydrate-active enzymes, which could help bacteria utilize different kinds of carbohydrate for survive. As shown in Fig. 3B, human disease-related Kyoto Encyclopedia of Genes and Genomes (KEGG) pathways annotation revealed that *K. pneumoniae* NKU_KlebA1 possesses drug resistance, cancer, infectious, immune, metabolic, and neurodegenerative diseases pathways, with antimicrobial drug resistance, bacterial infection disease, and cancers as three most dominant annotated pathways. These results provide the genetic level of evidence for *Klebsiella*'s plausible contribution to human diseases. Since there are multiple drug resistance and other human disease-related pathways in the genome of *Klebsiella*, the bloom of *Klebsiella* from AMX exposure would lead to the enrichment of the corresponding pathways. Furthermore, other human disease-related systems including pathogen-host

interactions, antibiotic resistance, virulence factors, and secretion systems were summarized in Fig. 3C-F, and details in supplemental Excel S2. The most dominant pathogen-host interaction was reduced virulence (63%), the most dominant drug resistance was efflux pump conferring antibiotic resistance (43%), and the two most dominant virulence factors were iron uptake system (nonspecific virulence factors, 33%) and adherence (offensive virulence factors, 26%). For secretion systems, NKU_KlebA1 carries all genes belonging to the Type II Secretion System, Sec-SRP Secretion System and Tat Secretion System, and some genes belonging to Type VI Secretion System and Type I Secretion System.

AMX exposure significantly increased the virulence of *Klebsiella* and its molecular mechanisms

To investigate the AMX's influence on virulence of *Klebsiella*, 8 *Klebsiella* strains were also isolated from AMX-free control sample C-A2 (i.e., before AMX exposure) for comparison. Virulence phenotypes including biofilm formation, serum resistance and animal toxicology of all the 16 *Klebsiella* isolates were evaluated by crystal violet assay, serum bactericidal assay, and *G. mellonella* infection assay, respectively. The results demonstrated that *Klebsiella* strains isolated from AMX exposed sample had stronger biofilm formation ($p < 0.001$, Fig. 4A), serum resistance ($p< 0.01$, Fig. 4B), and *G. mellonella* inhibition capacities ($p < 0.05$, Fig. 4C) than those from AMX-free sample, suggesting AMX exposure dramatically increased the virulence of *Klebsiella*.

The phylogenetic tree of all isolated *Klebsiella* species based on 16S rRNA gene identification revealed that the *Klebsiella* NKU_Kleb8 (isolated from AMX-free sample C-A2) and NKU_KlebA1 (isolated from AMX exposed sample AMX-A2) were within a close genetic distance (Fig. 4D). Further, the whole-genome analysis of strains NKU_KlebA1 and NKU_Kleb8 also implied that these two strains shared only 8 single nucleotide polymorphisms (SNPs) and 471 insertion-deletions (InDels) (as detailed in supplemental Excel S3A). Furthermore, multilocus sequence typing (MLST) confirmed these two strains both belong to ST22, and average nucleotide identity (ANI) analysis demonstrated the nucleotide identity of these two strains were 99.97% (Fig. S2). Therefore, these results collectively suggested that NKU_KlebA1 might be the evolved strain from NKU_Kleb8 exposed to AMX. Using methods described above, we also found NKU_KlebA1 had a substantially higher level of virulence than NKU_Kleb8 in the term of biofilm formation, serum resistance and *G. mellonella* infection (Fig. 4E-G).

To further confirm that AMX exposure could significantly increase the virulence of *Klebsiella*, a strain named NKU_Kleb8A7 was evolved from strain NKU_Kleb8 exposure to 600 mg/day AMX for seven days, and results of virulence shown in Fig. 4E-G also manifested a significantly higher virulence of NKU_Kleb8A7 than NKU_Kleb8 ($p < 0.01$). We subsequently analyzed the virulence factors of the wild strain NKU_Kleb8 and two evolved strains NKU_KlebA1 and NKU_Kleb8A7. Compared with NKU_Kleb8, 8 new virulence factor genes emerged and 39 genes appeared SNP and InDel sites in NKU_KlebA1 (Excel S3B), and 30 new virulence factor genes emerged and 251 genes mutated with SNP and InDel sites in NKU_Kleb8A7 (Excel S3C), as detailed in supplemental Excel S3D and S3E. The detailed genomic mutations of four major classes of virulence factors in NKU_KlebA1 and NKU_Kleb8A7 were shown in Table 1. In detail, capsule virulence factor *cpsI* appeared InDel sites in NKU_KlebA1, *cpsO* and *wcbB* were

new emerged virulence factors in NKU_Kleb8A7, and all the others appeared SNP sites in NKU_Kleb8A7. For fimbriae virulence factors, *lpfC*, *pilB*, and *pilG* had genomic mutations in both evolved strains, and most virulence factors appeared InDel sites in NKU_KlebA1 but appeared SNP sites in NKU_Kleb8A7. LPS virulence factor *gtrB* mutated in both strains, and all the others were new emerged genes or appeared SNP sites in NKU_Kleb8A7. Mutations in *fepA, EntD* and *iutA* were also observed in both strains, and all the other siderophores virulence factors were new emerged genes or appeared SNP sites in NKU_Kleb8A7. Owing to their importance in protein function and disease causing, the potential unintended consequence of these mutations needs a special concern.

Discussion

Enrichment of *Klebsiella* and human disease-related pathways in intestinal microbiota after AMX exposure

Using designed SHIME model, the impact of AMX on the human intestinal microbiota was investigated by high-throughput sequencing approach in this study. *Bacteriodetes, Proteobacteria, Synergistetes*, and *Firmicutes* were identified as four predominant phyla in simulated gut microbiota. Similar bacterial communities have been reported in some fecal samples and SHIME models in previous studies [26-28]. In addition, the inconsistent bacterial phyla were identified in three different colon regions, providing further evidence that colon regions play important roles in shaping the structure of gut microbiota [17]. The observed enrichment of bacteria in *Klebsiella* after exposure to AMX was consistent with previous findings that β-lactam antibiotics, vancomycin, and sulfonamide antibiotics exposure could increase the *Klebsiella* population [10-13]. To our best knowledge, there is currently just one study noticed that AMX increased the abundance of *Klebsiella* in human intestinal microbiota, while unfortunately no further mechanistic explanation and accompanying health consequences were provided [23]. Although *Klebsiella* genus is commensal organisms in the human gut, fecal carriage of extended-spectrum β-lactamase-producing *K. pneumoniae* had been found as a significant risk factor for infection as early as 20 years ago [29]. Moreover, increased researches have also confirmed that human gut was a major reservoir for *Klebsiella*, and the bloom of those intestinal *Klebsiella* may cause the various infections in different body parts of human-being [30, 31]. For example, pneumonia, Crohn's disease, colitis, cystitis, wound infections, and liver abscess have been found to relate to the bloom of *Klebsiella* in the human gut [11, 32]. Antibiotic-resistant *Klebsiella* isolated in this study belong to sequence type 22 (ST22), a rare sequence type described in two previous studies [33, 34]. Above studies confirmed *Klebsiella* (ST22) could cause pneumonia and display multidrug resistance.

As with abundance of *Klebsiella*, human disease-related pathways in different colon regions exhibited similar change trends as the function of time. More importantly, significant positive correlations between human disease-related pathways and *Klebsiella* suggested that the *Klebsiella* bloom caused by AMX might contribute to the increase of these pathways. It is known that frequent use of AMX in medicine may cause the development and spread of ARB and ARGs in human gut microbiome [25, 35, 36]. As expected, β-lactam resistance pathways increased after β-lactam antibiotic AMX exposure and its nice positive

correlation with *Klebsiella* abundance was also consistent with the fact that *Klebsiella* spp are intrinsic resistance to β-lactam antibiotics via producing β-lactamase (Fig. 2) [37]. Unexpected increases of vancomycin and CAMP resistance pathways with the increasing of *Klebsiella* indicated the potential co-selection on different antibiotic resistance from AMX [38]. In the present study, human disease-related pathways like cancer, infectious diseases, metabolic diseases, and neurosurgery diseases were all strongly associated with the *Klebsiella* abundance, which is also supported by some previous studies [39-43]. Taken cancer and infectious disease as examples, *Klebsiella* spp. has been considered as one of the most concerning pathogens frequently involved in infections of cancer patients and led to high mortality [40, 44]. Infectious diseases such as urinary tract infection, pyelonephritis, urosepsis, wound infection, cytomegalovirus disease, and pneumonia had been extensively reported to associate with the *Klebsiella* [11, 32]. KEGG pathways with human disease annotation by whole-genome analysis shown in this paper confirmed *Klebsiella*'s plausible contribution to human diseases, and many researchers have also revealed that *Klebsiella* possesses intrinsic virulence factor, antibiotic resistance, pathogen host interactions and secretion system, which determine their negative effects on human health [45-47].

AMX effects were colon region-different and persistent

In this study, *Klebsiella* was found to be more significantly enriched in ascending colon than the other two colon-regions (Fig. 1), which was in keeping with previous reports for the changes of intestinal microbiota in exposure to the antibiotic mixtures and other toxic compounds like chlorpyrifos and arsenic [17, 28, 48]. These “SHIME-compartment” specific effects could be due to the inconsistent compounds biodegradation, gut microbiome community, and pH in different colon regions [17, 28, 48]. Meanwhile, the largest increase of predicted human disease-related pathways was also shown in ascending colon after AMX exposure (Fig. 2), which clarified that the primary effect observed at the level of the microbiota could also be identified at the genomic and metabolic level, as reported in other researches [49, 50]. Furthermore, these AMX effects were still evident for at least two weeks after the AMX discontinuance although the resilient reductions of *Klebsiella* and human disease-related pathways were observed. A recent research revealed that AMX mediated opportunistic pathogen *Escherichia/Shigella* blooms persisted 42 days after the interruption of antibiotic therapy [22]. Similar phenomenon was also reported by Zwittink and colleagues, who also discovered that 5 days treatment with AMX and ceftazidime combinations allowed *Enterococcus* to thrive and remain dominant for up to two weeks and caused *Bifidobacterium* abundance to remain decreased till postnatal week six after antibiotic treatment discontinuation [51]. Therefore, our results demonstrated the serious negative side-effect of AMX could be persistent and colon region-different, which should be considered as an important aspect of the risk assessment for AMX prescription.

AMX dramatically increased the virulence of *Klebsiella* by mutations of virulence factors

Our finding that seven days of 600 mg/day AMX acclimated NKU_Kleb8A7 had significantly higher virulence than NKU_Kleb8 supported the hypothesis that AMX exposure could significantly increase the virulence of *Klebsiella*, which has not been reported yet. However, antibiotics chloramphenicol and

erythromycin had been found to increase the virulence of *Acinetobacter baumannii* by increasing the production of the K locus exopolysaccharide (one important component of biofilm) [52]. Treatment with ciprofloxacin could enhance the expression of virulence genes of opportunistic pathogen *Salmonella typhimurium,* resulting in the increased virulence [53]. These results indicated that the significantly increased virulence of *Klebsiella* revealed in our research might also be attributed to the improved virulence genes expression. It was mentioned earlier that the inherent resistance to β-lactam already poses a significant therapeutic challenge for *Klebsiella* infections, the AMX-induced virulence increasing phenomenon found in this study undoubtedly further increase its health risk [54-56].

K. pneumoniae employs four major classes of virulence factors (fimbriae, lipopolysaccharide (LPS), capsule, and siderophores) to protect itself from the inhibition of host immune [57]. Fimbriae virulence factors are important mediators for the adhesion and biofilm formation of *K. pneumoniae*. In this study, fimbriae virulence factors of *pilB*, *pilG*, and *fimD* were all mutated in both evolved strains NKU_KlebA1 and NKU_Kleb8A7 which may substantially increase the biofilm formation ability of *K. pneumoniae*, resulting in increasing their virulence [58-61]. LPS and capsule virulence factors have been suggested as the main deterrent to complement-mediated lysis [62, 63]. O antigen is the outermost subunit of LPS and has important roles in protecting against complement. Lack of O-antigen may render *K. pneumoniae* sensitive to complement-mediated killing in the bloodstream, thus making the strain less virulent [64]. *GtrB* encodes bactoprenol glucosyl transferase, which was necessary to express O-antigen in *Shigella flexneri*, and its mutation in both evolved strains may attribute to their increasing serum resistance ability [65]. Moreover, the new emerged O-antigen related genes such as *wzt*, *wzx*, *manB*, and *manC* in NKU_Kleb8A7 putatively improve O-antigen's deterrent to complement-mediated lysis. *Cps* gene cluster is involved in the production of the capsule polymer, and acapsular strains are easier detected by opsonophagocytosis and more likely killed in serum via the alternative complement pathway, thus the mutated *cpsB* and *cpsI* may be the important mediators of increasing serum resistance [66, 67]. Siderophores are necessary virulence factors for *K. pneumoniae* to acquire iron from the host in order to survive and propagate during infection, and the production of more than one siderophore help avoiding neutralization of one siderophore by the host [68]. Enterobactin is the primary siderophore used by *K. pneumoniae*, *fepA* is required for its biosynthesis and *entD* is necessary for its transport, the mutations of these two genes in both evolved strains may substantially increased their affinity for iron [69]. Similaly, *iutA* that encods aerobactin was also mutated in both evolved strains, which maybe a very important factor for *G. mellonella* infection [70]. Moreover, the new emerged yersiniabactin synthesis and secretion genes such as *irp*1, *irp*2, *fyuA*, and *ybtT* in NKU_Kleb8A7, as well as salmochelin formation related gene *iroN* and *iroE* putatively attributed to its stronger infection ability to *G. mellonella* [71, 72].

Several other virulence factors were recently identified as being important for virulence of *K. pneumoniae*. It's well-known that many human pathogens use type II secretion system to secrete toxins and enzymes to damage specific tissues, resulting in cell damage and disease [73, 74]. Virulence factor g*spG*, which encodes the putative type II secretion protein, was confirmed to be mutated after AMX exposure in both evolved strains of NKU_KlebA1 and NKU_Kleb8A7. As one important subassembly of type II secretion system, pseudopilin *gspG* family was reported to drive folded proteins across the outer membrane in a

piston-like manner. The expression of *gspG* from *lacZP* in *E. coli* had been reported to produce *gspG*-specific antiserum recognized protein [75]. The C terminus of protein G represented a permissive site which is important for its function, the mutations shown in this study would affect its combination with proteins secreted and antibody in serum, which may then cause the increasing survival of *Klebsiella* when exposure to serum or *G. mellonella* infection [76]. Pathogenic species also use type III secretion systems to inject toxins into attacking immune cells, the mutated genes such as *vscN* and *exsA* may upregulate expression of type III secretion systems in NKU_Kleb8A7 and then improve its survival and affection ability [77, 78]. ABC iron transport system is also identified important for *K. pneumoniae* virulence, which is involved in the acquisition of iron [79]. This kind of virulence factor genes *fbpC* and *hitC* were confirmed to mutate after AMX exposure in both evolved strains, which may enhance their infection ability in *G. mellonella*. However, further studies are needed to verify whether the mutations of the above virulence factors is related to the increased virulence of *K. pneumoniae* observed in this study.

Conclusions

Exposure to AMX increased the abundances of *Klebsiella* and human disease-related pathways in simulated human gut microbiota and the most significant enhancement effect was observed for ascending colon. Meanwhile, the significant increase in *Klebsiella* population could persistent for at least two weeks after AMX discontinuance. The increased predicted functional pathways were positively associated with *Klebsiella* and whole-genome analysis also confirmed *Klebsiella* strains indeed carry these human disease-related KEGG pathways. Moreover, exposure to AMX dramatically enhanced the virulence of *Klebsiella* including biofilm formation, serum resistance, and *G. mellonella* infection. Genome sequence comparison analysis of strain NKU_Kleb8 (isolated from SHIME before AMX exposure) with the strain NKU_KlebA1 (isolated from SHIME after AMX exposure) and NKU_Kleb8A7 (evolved from NKU_Kleb8 after AMX exposure) revealed that the increased virulence may be attributed to the mutations of four major virulence factors relevant to fimbriae, LPS, capsule, and siderophores. Our results may open up new perspectives for assessing the direct effects of AMX on the intestinal microbiota—a key “organ” in individual health. Further analysis of the increased and evolved *Klebsiella in vivo* should be conducted for better understanding the effects of AMX on human health.

Materials And Methods

SHIME model start up and samples collection

The constructed SHIME was formed by five double-jacketed reactors simulating the stomach, small intestine, ascending colon, transverse colon, and descending colon, respectively (Fig. 1A). The last three reactors were inoculated with a mixture of fecal microbiota from a healthy adult volunteer, who did not suffer from gastrointestinal diseases or take antibiotics in the past six months [28, 80]. During the first two weeks of the experiment, AMX-free nutritional medium was added to the reactors to stabilize the microbial community. After this period, the SHIME was sequentially exposed to AMX-free nutritional medium for another one week and followed by nutritional medium + 600 mg/day AMX for one week, and

AMX-free nutritional medium for two weeks. The details of the SHIME system and the startup process are summarized in the Supporting Material.

Liquid samples (mixtures of fecal microbiota with SHIME feed) were collected from simulated ascending colon, transverse colon and descending colon vessels at six time points of 14, 21, 24, 28, 35, and 42 day, as detailed in Fig. 1A. Based on the situation of AMX exposure, these samples can be classified into three groups. Specifically, the first group of samples were collected after stabilization of SHIME setup for two weeks (C-A1, C-T1, and C-D1 from ascending colon, transverse colon and descending colon, respectively) and before the AMX administration (i.e., C-A2, C-T2, and C-D2). The second group sampled after the administration of AMX for three days (AMX-A1, AMX-T1, and AMX-D1) and seven days (AMX-A2, AMX-T2, and AMX-D2). Finally, the third group of samples were collected after the discontinuance of AMX for one week (R-A1, R-T1, and R-D1) and two weeks (R-A2, R-T2 and R-D2). Samples were stored at −80 °C for further analyses.

16S rRNA gene sequencing and analysis

Microbial DNA was extracted from samples using the E.Z.N.A. stool DNA Kit (Omega, USA) according to manufacturer's protocols. The V3-V4 region of the bacterial 16S rRNA gene were amplified by polymerase chain reaction (PCR). The raw reads were deposited into the NCBI Sequence Read Archive (SRA) database with the accession number of SRR9330193-SRR9330210. The details of bacterial DNA extraction and PCR amplification of 16S rRNA gene were described in the Supporting Material.

Raw Illumina fastq files were demultiplexed, quality-filtered, and analyzed using Quantitative Insights Into Microbial Ecology (QIIME) [81]. Sequences that were shorter than 55 bp, contained primer mismatches, ambiguous bases or uncorrectable barcodes, were removed. 16S rRNA gene sequences were assigned to operational taxonomic units (OTUs) using UCLUST with a threshold of 97% pairwise identity, and then classified taxonomically using the Ribosomal Database Project (RDP) classifier 2.0.1 [82].

Functional predictions of microbial community were performed to visualize the distribution of human disease-related pathways in the three parts of colon with different treatment using Phylogenetic Investigation of Communities by Reconstruction of Unobserved States (PICRUSt) on closed-reference OTUs with 97% identity based on the Greengenes database (v13.5) [83]. The OTUs were normalized on PICRUSt and used for the prediction of KEGG orthologs (KOs).

LEfSe analysis was served to determine bacterial taxa that significantly differed between the control and AMX exposure group using the Galaxy application tool (http://huttenhower.sph.harvard.edu/galaxy/) with a linear discriminant analysis, where the cutoff score is of 3.0 and a p of < 0.05 for statistical significance [84]. These analyses were conducted by Guangzhou Gene Denovo Co., Ltd (Guangzhou, China).

Qualitative PCR, Biofilm formation, serum killing and *G. mellonella* infection assay of *Klebsiella* isolated strains

A total of 16 *Klebsiella* strains were isolated from ascending colon samples by a *Klebsiella*-specific MacConkey-inositol-adonitol-carbenicillin medium, as described by Gao et al [85]. Among them, eight were isolated from sample C-A2 (before AMX administration) and the others were from AMX-A2 (after AMX exposure). DNA was extracted from *Klebsiella* strains using the Wizard Genomic DNA Purification Kit (Promega, USA) according to manufacturer's protocols. 16S rRNA gene identification conducted by BGI Tech Solutions Beijing Liuhe Co., Ltd (Beijing, China) also confirmed the isolated strains were *Klebsiella*. The phylogenetic tree of these *Klebsiella* strains was conducted by MEGA X [86]. 5 ARGs (*bl2b_tem1*, *bl2be_shv2*, *arna*, *rosb*, and *vang*) related to drug resistance pathways from the isolated strains were confirmed using Qualitative PCR on a Biometra T100 gradient (Biometra) with the primers listed in Table S3 [87].

Biofilms formation were assayed using the standard crystal violet quantification assay described by O'Toole and associates [88]. Serum-killing assay was performed based on the method described by Rosen and associates [89]. *G. mellonella* infection assay was conducted as described by McLaughlin and associates [90]. Details of phylogenetic tree establishment, Qualitative PCR, biofilm formation, serum killing and *G. mellonella* infection assay procedures are described in the Supporting Material.

Genome sequencing and analysis of *Klebsiella*

DNA was extracted from *Klebsiella* strains using the Wizard Genomic DNA Purification Kit (Promega, USA) according to manufacturer's protocols. Whole genome of *Klebsiella* strain NKU_Kleb8 (isolated from ascending colon before AMX administration), NKU_KlebA1 (isolated from ascending colon after AMX exposure), and NKU_Kleb8A7 (evolved from strain NKU_Kleb8 exposure to AMX) were sequenced. Details of whole genome sequencing and assembling are described in the Supporting Material. The Scaffolds of NKU_Kleb8, NKU_KlebA1 and NKU_Kleb8A7 were deposited into the NCBI Genomes database with the accession numbers in GenBank of no.VKKD00000000, no.CP041648-CP041649, and no.CP041644-CP041645, respectively.

The whole-genome of *Klebsiella* strain NKU_KlebA1 was analyzed on the free online platform of Majorbio I-Sanger Cloud Platform (www.i-sanger.com). For genome pair of NKU_Kleb8 and NKU_KlebA1, the value of ANI was calculated according to sequence-based comparisons by Goris et al. [91]. Multilocus sequence typing (MLST) of these two strains were determined using the Institut Pasteur MLST databases.

SNP mutations between NKU_Kleb8A7 and NKU_KlebA1 with NKU_Kleb8 were obtained by sequence alignment using the software package MUMmer version 3.23 [92]. After the alignment of LASTZ (http://www.bx.psu.edu/~rsharris/lastz/), the best match results (less than 10 bp) were extracted by using axtBest to obtain the preliminary InDel results [93]. The 150 bp (3×SD) from upstream and downstream of the reference sequence InDel sites were aligned and validated with the sample sequencing reads by BWA software [94]. After filtering, the reliable InDel sites were obtained. These analyses were conducted by BioMarker Technology Co., Ltd (Beijing, China).

Data analysis

Results are expressed as mean values and standard deviations. The statistical analysis was performed with SPSS 17.0 software. The T-tests were conducted to compare the difference between groups and all statistical tests were two-tailed. Statistical significance was set at three different levels (*$p < 0.05$, **$p < 0.01$, and ***$p < 0.001$). Spearman test for correlation analysis between gene numbers of human disease-related pathways and the *Klebsiella* abundance were performed in R with the vegan package.

Abbreviations

AMX: amoxicillin; ANI: average nucleotide identity; CAMP: cationic antimicrobial peptide; CFU: colony-forming units; CRISPR/Cas: clustered regularly interspaced palindromic repeats/CRISPR-associated proteins; InDels: insertion-deletions; KEGG: Kyoto Encyclopedia of Genes and Genomes; Kos: KEGG orthologs; LB: Luria-Bertani; LEfSe: linear discriminant analysis effect size; LPS: lipopolysaccharide; MLST: multilocus sequence typing; OUT: operational taxonomic units; PBS: Phosphate Buffered Saline; PCR: polymerase chain reaction; PICRUSt: Phylogenetic Investigation of Communities by Reconstruction of Unobserved States; QIIME: Quantitative Insights Into Microbial Ecology; RDP: Ribosomal Database Project; SHIME: simulator of the human intestinal microbial ecosystem; SNPs: single nucleotide polymorphisms; SRA: Sequence Read Archive; USA: the United States of America;

Declarations

Acknowledgments

The authors express the sincerest thanks to Professor Bing Wu at Nanjing University, for the guidance of constructing SHIME model.

Funding

This study was supported by the Key projects of the National Natural Science Foundation of China (41831287), China National Funds for Distinguished Young Scientists (41525013), and National Natural Science Foundation of China (31870351, 31670509, 41977367, 41807483, 41703088, and 21607016).

Availability of data and materials

The datasets and scripts developed and generated in this manuscript are included within the manuscript and its supporting files.

Consent for publication

Not applicable.

Authors' contributions

LL carried out the laboratory work, analyzed the data, and wrote the manuscript. ZC and QW revised the manuscript and provided financial support. JS, WB, SW, YG, HL, HQ, SZ and JY carried out the laboratory work. YX provided financial support. DM and YL guided the laboratory work and revised this manuscript, and provided financial support. All authors read and approved the final manuscript.

Ethics approval and consent to participate

The study was approved by the Biomedical Ethics Committees of Nankai University. The participant has given written informed consent to understand the study purpose, procedures, risks, benefits, and rights.

Competing interests

The authors declare that they have no competing interests.

References

1. Khan I, Yasir M, Azhar EI, Kumosani T, Barbour EK, Bibi F, et al. Implication of gut microbiota in human health. CNS Neurol Disord Drug Targets. 2014;13(8):1325-33.
2. Celluzzi A, Masotti A. How our other genome controls our epi-genome. Trends Microbiol. 2016;24(10):777-87.
3. Sender R, Fuchs S, Milo R. Are we really vastly outnumbered? Revisiting the ratio of bacterial to host cells in humans. Cell. 2016;164(3):337-40.
4. van de Guchte M, Blottiere HM, Dore J. Humans as holobionts: implications for prevention and therapy. Microbiome. 2018;6.
5. Yatsunenko T, Rey FE, Manary MJ, Trehan I, Dominguez-Bello MG, Contreras M, et al. Human gut microbiome viewed across age and geography. Nature. 2012;486(7402):222-7.
6. Blaser MJ. Antibiotic use and its consequences for the normal microbiome. Science. 2016;352(6285):544-5.
7. Ianiro G, Tilg H, Gasbarrini A. Antibiotics as deep modulators of gut microbiota: between good and evil. Gut. 2016;65(11):1906-15.
8. Stecher B, Maier L, Hardt WD. 'Blooming' in the gut: how dysbiosis might contribute to pathogen evolution. Nat Rev Microbiol. 2013;11(4):277-84.
9. Barraud O, Peyre M, Couve-Deacon E, Chainier D, Bahans C, Guigonis V, et al. Antibiotic resistance acquisition in the first week of life. Front Microbiol. 2018;9:1467.
10. Gibson MK, Wang B, Ahmadi S, Burnham CA, Tarr PI, Warner BB, et al. Developmental dynamics of the preterm infant gut microbiota and antibiotic resistome. Nat Microbiol. 2016;1:16024.
11. Schneditz G, Rentner J, Roier S, Pletz J, Herzog KA, Bucker R, et al. Enterotoxicity of a nonribosomal peptide causes antibiotic-associated colitis. Proc Natl Acad Sci U S A. 2014;111(36):13181-6.
12. Isaac S, Scher JU, Djukovic A, Jimenez N, Littman DR, Abramson SB, et al. Short- and long-term effects of oral vancomycin on the human intestinal microbiota. J Antimicrob Chemother.

2017;72(1):128-36.

13. Powis K, Souda S, Lockman S, Ajibola G, Bennett K, Leidner J, et al. Cotrimoxazole prophylaxis was associated with enteric commensal bacterial resistance among HIV-exposed infants in a randomized controlled trial, Botswana. J Int AIDS Soc. 2017;20(3):e25021.
14. El Hage R, Hernandez-Sanabria E, Calatayud Arroyo M, Props R, Van de Wiele T. Propionate-producing consortium restores antibiotic-induced dysbiosis in a dynamic *in vitro* model of the human intestinal microbial ecosystem. Front Microbiol. 2019;10:1206.
15. Ichim TE, Kesari S, Shafer K. Protection from chemotherapy- and antibiotic-mediated dysbiosis of the gut microbiota by a probiotic with digestive enzymes supplement. Oncotarget. 2018;9(56):30919-35.
16. Ladirat SE, Schuren FHJ, Schoterman MHC, Nauta A, Gruppen H, Schols HA. Impact of galacto-oligosaccharides on the gut microbiota composition and metabolic activity upon antibiotic treatment during *in vitro* fermentation. FEMS Microbiol Ecol. 2014;87(1):41-51.
17. Marzorati M, Vilchez-Vargas R, Bussche JV, Truchado P, Jauregui R, El Hage RA, et al. High-fiber and high-protein diets shape different gut microbial communities, which ecologically behave similarly under stress conditions, as shown in a gastrointestinal simulator. Mol Nutr Food Res. 2017;61(1):1600150.
18. Van de Wiele T, Van den Abbeele P, Ossieur W, Possemiers S, Marzorati M. The simulator of the human intestinal microbial ecosystem (SHIME®). In: Verhoeckx K, Cotter P, López-Expósito I, Kleiveland C, Lea T, Mackie A, et al., editors. The Impact of Food Bioactives on Health: in vitro and ex vivo models. Cham: Springer International Publishing; 2015, p. 305-17.
19. Marzorati M, Van de Wiele T. An advanced *in vitro* technology platform to study the mechanism of action of prebiotics and probiotics in the gastrointestinal tract. J Clin Gastroenterol. 2016;50:S124-S5.
20. Zapata HJ, Quagliarello VJ. The microbiota and microbiome in aging: Potential implications in health and age-related diseases. J Am Geriatr Soc. 2015;63(4):776-81.
21. Zhang Q, Ying G, Pan C, Liu Y, Zhao J. Comprehensive evaluation of antibiotics emission and fate in the river basins of China: source analysis, multimedia modeling, and linkage to bacterial resistance. Environ Sci Technol. 2015;49(11):6772-82
22. Pallav K, Dowd SE, Villafuerte J, Yang X, Kabbani T, Hansen J, et al. Effects of polysaccharopeptide from *Trametes versicolor* and amoxicillin on the gut microbiome of healthy volunteers: a randomized clinical trial. Gut Microbes. 2014;5(4):458-67.
23. Oh B, Kim BS, Kim JW, Kim JS, Koh SJ, Kim BG, et al. The effect of probiotics on gut microbiota during the *Helicobacter pylori* eradication: randomized controlled trial. Helicobacter. 2016;21(3):165-74.
24. Reijnders D, Goossens GH, Hermes GD, Neis EP, van der Beek CM, Most J, et al. Effects of gut microbiota manipulation by antibiotics on host metabolism in obese humans: a randomized double-blind placebo-controlled trial. Cell Metab. 2016;24(1):63-74.

25. Zaura E, Brandt BW, Teixeira de Mattos MJ, Buijs MJ, Caspers MP, Rashid MU, et al. Same exposure but two radically different responses to antibiotics: Resilience of the salivary microbiome versus long-term microbial shifts in feces. MBio. 2015;6(6):e01693-15.
26. Gao Z, Guo B, Gao R, Zhu Q, Qin H. Microbiota disbiosis is associated with colorectal cancer. Front Microbiol. 2015;6:20.
27. Li S, Zhang C, Gu Y, Chen L, Ou S, Wang Y, et al. Lean rats gained more body weight than obese ones from a high-fibre diet. Br J Nutr. 2015;114(8):1188-94.
28. Yu H, Wu B, Zhang X, Liu S, Yu J, Cheng S, et al. Arsenic metabolism and toxicity influenced by ferric iron in simulated gastrointestinal tract and the roles of gut microbiota. Environ Sci Technol. 2016;50(13):7189-97.
29. Pena C, Pujol M, Ricart A, Ardanuy C, Ayats J, Linares J, et al. Risk factors for faecal carriage of *Klebsiella pneumoniae* producing extended spectrum beta-lactamase (ESBL-KP) in the intensive care unit. J Hosp Infect. 1997;35(1):9-16.
30. Gorrie C, Mirceta M, Wick R, Edwards D, Thomson N, Strugnell R, et al. Gastrointestinal carriage is a major reservoir of *Klebsiella pneumoniae* infection in intensive care patients. Clin Infect Dis. 2017;65(2):208-15.
31. Wiener-Well Y, Rudensky B, Yinnon AM, Kopuit P, Schlesinger Y, Broide E, et al. Carriage rate of carbapenem-resistant *Klebsiella pneumoniae* in hospitalised patients during a national outbreak. J Hosp Infect. 2010;74(4):344-9.
32. Atarashi K, Suda W, Luo C, Kawaguchi T, Motoo I, Narushima S, et al. Ectopic colonization of oral bacteria in the intestine drives TH1 cell induction and inflammation. Science. 2017;358(6361):359-65.
33. Torres-Gonzalez P, Bobadilla-Del Valle M, Tovar-Calderon E, Leal-Vega F, Hernandez-Cruz A, Martinez-Gamboa A, et al. Outbreak caused by *Enterobacteriaceae* harboring NDM-1 metallo-beta-lactamase carried in an IncFII plasmid in a tertiary care hospital in Mexico City. Antimicrob Agents Chemother. 2015;59(11):7080-3.
34. Barrios H, Silva-Sanchez J, Reyna-Flores F, Sanchez-Perez A, Sanchez-Francia D, Aguirre-Torres JA, et al. Detection of a-NDM1-producing *Klebsiella pneumoniae* (ST22) clinical isolate at a pediatric hospital in Mexico. Pediatr Infect Dis J. 2014;33(3):335.
35. Canton R, Morosini MI. Emergence and spread of antibiotic resistance following exposure to antibiotics. FEMS Microbiol Rev. 2011;35(5):977-91.
36. Moore AM, Ahmadi S, Patel S, Gibson MK, Wang B, Ndao MI, et al. Gut resistome development in healthy twin pairs in the first year of life. Microbiome. 2015;3:27.
37. Viau RA, Hujer AM, Marshall SH, Perez F, Hujer KM, Briceño DF, et al. “Silent” dissemination of *Klebsiella pneumoniae* isolates bearing *K. pneumoniae* carbapenemase in a long-term care facility for children and young adults in Northeast Ohio. Clin Infect Dis. 2012;54(9):1314-21.
38. Pouwels KB, Freeman R, Muller-Pebody B, Rooney G, Henderson KL, Robotham JV, et al. Association between use of different antibiotics and trimethoprim resistance: going beyond the obvious crude

association. J Antimicrob Chemother. 2018;73(6):1700-7.

39. Kuang Y, Lu J, Li S, Li J, Yuan M, He J, et al. Connections between the human gut microbiome and gestational diabetes mellitus. Gigascience. 2017;6(8):1-12.
40. Zhu J, Liao M, Yao Z, Liang W, Li Q, Liu J, et al. Breast cancer in postmenopausal women is associated with an altered gut metagenome. Microbiome. 2018;6(1):136.
41. Li J, Zhao F, Wang Y, Chen J, Tao J, Tian G, et al. Gut microbiota dysbiosis contributes to the development of hypertension. Microbiome. 2017;5(1):14.
42. Shen Y, Xu J, Li Z, Huang Y, Yuan Y, Wang J, et al. Analysis of gut microbiota diversity and auxiliary diagnosis as a biomarker in patients with schizophrenia: a cross-sectional study. Schizophr Res. 2018;197:470-7.
43. Zhu Q, Dupont CL, Jones MB, Pham KM, Jiang ZD, DuPont HL, et al. Visualization-assisted binning of metagenome assemblies reveals potential new pathogenic profiles in idiopathic travelers' diarrhea. Microbiome. 2018;6(1):201.
44. Freire M, Pierrotti L, Filho H, Ibrahim K, Magri A, Bonazzi P, et al. Infection with *Klebsiella pneumoniae* carbapenemase (KPC)-producing *Klebsiella pneumoniae* in cancer patients. Eur J Clin Microbiol Infect Dis. 2015;34(2):277-86.
45. Chung The H, Karkey A, Pham Thanh D, Boinett C, Cain A, Ellington M, et al. A high-resolution genomic analysis of multidrug-resistant hospital outbreaks of *Klebsiella pneumoniae*. EMBO Mol Med. 2015;7(3):227-39.
46. Long S, Olsen R, Eagar T, Beres S, Zhao P, Davis J, et al. Population genomic analysis of 1,777 extended-spectrum beta-lactamase-producing isolates, Houston, Texas: unexpected abundance of clonal group 307. MBio. 2017;8(3):e00489-17.
47. Runcharoen C, Moradigaravand D, Blane B, Paksanont S, Thammachote J, Anun S, et al. Whole genome sequencing reveals high-resolution epidemiological links between clinical and environmental *Klebsiella pneumoniae*. Genome Med. 2017;9(1):6.
48. Reygner J, Joly Condette C, Bruneau A, Delanaud S, Rhazi L, Depeint F, et al. Changes in composition and function of human intestinal microbiota exposed to chlorpyrifos in oil as assessed by the SHIME® model. Int J Environ Res Public Health. 2016;13(11):1088.
49. Garcia-Villalba R, Vissenaekens H, Pitart J, Romo-Vaquero M, Espin JC, Grootaert C, et al. Gastrointestinal simulation model TWIN-SHIME shows differences between human urolithin-metabotypes in gut microbiota composition, pomegranate polyphenol metabolism, and transport along the intestinal tract. J Agric Food Chem. 2017;65(27):5480-93.
50. Wang Y, Rui M, Nie Y, Lu G. Influence of gastrointestinal tract on metabolism of bisphenol A as determined by *in vitro* simulated system. J Hazard Mater. 2018;355:111-8.
51. Zwittink RD, Renes IB, van Lingen RA, van Zoeren-Grobben D, Konstanti P, Norbruis OF, et al. Association between duration of intravenous antibiotic administration and early-life microbiota development in late-preterm infants. Eur J Clin Microbiol Infect Dis. 2018;37(3):475-83.

52. Geisinger E, Isberg R. Antibiotic modulation of capsular exopolysaccharide and virulence in *Acinetobacter baumannii*. PLoS Pathog. 2015;11(2):e1004691.
53. Diard M, Sellin M, Dolowschiak T, Arnoldini M, Ackermann M, Hardt W. Antibiotic treatment selects for cooperative virulence of *Salmonella typhimurium*. Curr Biol. 2014;24(17):2000-5.
54. Gu D, Dong N, Zheng Z, Lin D, Huang M, Wang L, et al. A fatal outbreak of ST11 carbapenem-resistant hypervirulent *Klebsiella pneumoniae* in a Chinese hospital: a molecular epidemiological study. Lancet Infect Dis. 2018;18(1):37-46.
55. Munoz-Price LS, Poirel L, Bonomo RA, Schwaber MJ, Daikos GL, Cormican M, et al. Clinical epidemiology of the global expansion of *Klebsiella pneumoniae* carbapenemases. Lancet Infect Dis. 2013;13(9):785-96.
56. Zhang Y, Zhao C, Wang Q, Wang X, Chen H, Li H, et al. High prevalence of hypervirulent *Klebsiella pneumoniae* infection in China: geographic distribution, clinical characteristics, and antimicrobial resistance. Antimicrob Agents Chemother. 2016;60(10):6115-20.
57. Paczosa MK, Mecsas J. *Klebsiella pneumoniae*: going on the offense with a strong defense. Microbiol Mol Biol Rev. 2016;80(3):629-61.
58. Adler A, Khabra E, Chmelnitsky I, Giakkoupi P, Vatopoulos A, Mathers AJ, et al. Development and validation of a multiplex PCR assay for identification of the epidemic ST-258/512 KPC-producing *Klebsiella pneumoniae* clone. Diagn Microbiol Infect Dis. 2014;78(1):12-5.
59. Struve C, Bojer M, Krogfelt KA. Characterization of *Klebsiella pneumoniae* type 1 fimbriae by detection of phase variation during colonization and infection and impact on virulence. Infect Immun. 2008;76(9):4055-65.
60. Lau HY, Clegg S, Moore TA. Identification of *Klebsiella pneumoniae* genes uniquely expressed in a strain virulent using a murine model of bacterial pneumonia. Microb Pathog. 2007;42(4):148-55.
61. Maroncle N, Balestrino D, Rich C, Forestier C. Identification of *Klebsiella pneumoniae* genes involved in intestinal colonization and adhesion using signature-tagged mutagenesis. Infect Immun. 2002;70(8):4729-34.
62. Clements A, Gaboriaud F, Duval JF, Farn JL, Jenney AW, Lithgow T, et al. The major surface-associated saccharides of *Klebsiella pneumoniae* contribute to host cell association. PLoS One. 2008;3(11):e3817.
63. Fang CT, Chuang YP, Shun CT, Chang SC, Wang JT. A novel virulence gene in *Klebsiella pneumoniae* strains causing primary liver abscess and septic metastatic complications. J Exp Med. 2004;199(5):697-705.
64. Yeh KM, Chiu SK, Lin CL, Huang LY, Tsai YK, Chang JC, et al. Surface antigens contribute differently to the pathophysiological features in serotype K1 and K2 *Klebsiella pneumoniae* strains isolated from liver abscesses. Gut Pathog. 2016;8:4.
65. Dharmasena MN, Osorio M, Takeda K, Stibitz S, Kopecko DJ. Stable chromosomal expression of *Shigella flexneri* 2a and 3a O-antigens in the live *Salmonella* oral vaccine vector Ty21a. Clin Vaccine Immunol. 2017;24(12):e00181-17.

66. Cortes G, Borrell N, de Astorza B, Gomez C, Sauleda J, Alberti S. Molecular analysis of the contribution of the capsular polysaccharide and the lipopolysaccharide O side chain to the virulence of *Klebsiella pneumoniae* in a murine model of pneumonia. Infect Immun. 2002;70(5):2583-90.
67. Standish AJ, Salim AA, Zhang H, Capon RJ, Morona R. Chemical inhibition of bacterial protein tyrosine phosphatase suppresses capsule production. PLoS One. 2012;7(5):e36312.
68. Bachman MA, Lenio S, Schmidt L, Oyler JE, Weiser JN. Interaction of lipocalin 2, transferrin, and siderophores determines the replicative niche of *Klebsiella pneumoniae* during pneumonia. MBio. 2012;3(6):e00224-11.
69. El Fertas-Aissani R, Messai Y, Alouache S, Bakour R. Virulence profiles and antibiotic susceptibility patterns of *Klebsiella pneumoniae* strains isolated from different clinical specimens. Pathol Biol (Paris). 2013;61(5):209-16.
70. Khalil MAF, Hager R, Abd-El Reheem F, Mahmoud EE, Samir T, Moawad SS, et al. A study of the virulence traits of carbapenem-resistant *Klebsiella pneumoniae* isolates in a *Galleria mellonella* model. Microb Drug Resist. 2019.
71. Lawlor MS, O'Connor C, Miller VL. Yersiniabactin is a virulence factor for *Klebsiella pneumoniae during* pulmonary infection. Infect Immun. 2007;75(3):1463-72.
72. Muller S, Valdebenito M, Hantke K. Salmochelin, the long-overlooked catecholate siderophore of *Salmonella*. BioMetals. 2009;22(4):691-5.
73. Sandkvist M. Type II secretion and pathogenesis. Infect Immun. 2001;69(6):3523-35.
74. Cianciotto NP. Type II secretion: a protein secretion system for all seasons. Trends Microbiol. 2005;13(12):581-8.
75. Francetic O, Pugsley A. The cryptic general secretory pathway (gsp) operon of *Escherichia coli* K-12 encodes functional proteins. J Bacteriol. 1996;178(12):3544-9.
76. Cisneros D, Bond P, Pugsley A, Campos M, Francetic O. Minor pseudopilin self-assembly primes type II secretion pseudopilus elongation. EMBO J. 2012;31(4):1041-53.
77. Marsden AE, Intile PJ, Schulmeyer KH, Simmons-Patterson ER, Urbanowski ML, Wolfgang MC, et al. Vfr directly activates exsA transcription to regulate expression of the *Pseudomonas aeruginosa* type III secretion system J Bacteriol. 2016;198(9):1442-50.
78. Bulir DC, Waltho DA, Stone CB, Mwawasi KA, Nelson JC, Mahony JB. *Chlamydia pneumoniae* CopD translocator protein plays a critical role in type III secretion (T3S) and infection. PLoS One. 2014;9(6):e99315.
79. Chen YT, Chang HY, Lai YC, Pan CC, Tsai SF, Peng HL. Sequencing and analysis of the large virulence plasmid pLVPK of *Klebsiella pneumoniae* CG43. Gene. 2004;337:189-98.
80. Yin N, Zhang Z, Cai X, Du H, Sun G, Cui Y. *In vitro* method to assess soil arsenic metabolism by human gut microbiota: Arsenic speciation and distribution. Environ Sci Technol. 2015;49(17):10675-81.

81. Caporaso JG, Kuczynski J, Stombaugh J, Bittinger K, Bushman FD, Costello EK, et al. QIIME allows analysis of high-throughput community sequencing data. Nat Methods. 2010;7(5):335-6.
82. Edgar RC. Search and clustering orders of magnitude faster than BLAST. Bioinformatics. 2010;26(19):2460-1.
83. Langille MG, Zaneveld J, Caporaso JG, McDonald D, Knights D, Reyes JA, et al. Predictive functional profiling of microbial communities using 16S rRNA marker gene sequences. Nat Biotechnol. 2013;31(9):814-21.
84. Segata N, Izard J, Waldron L, Gevers D, Miropolsky L, Garrett WS, et al. Metagenomic biomarker discovery and explanation. Genome Biol. 2011;12(6):R60.
85. Gao H, Gao QL, Zhang X, Guan C, Luo MH, Zhang HB, et al. Improved medium for detection of *Klebsiella* in powdered milk. J Food Saf. 2010;30(1):12-23.
86. Kumar S, Stecher G, Li M, Knyaz C, Tamura K. MEGA X: molecular evolutionary genetics analysis across computing platforms. Mol Biol Evol. 2018;35(6):1547-9.
87. Yang F, Mao D, Zhou H, Wang X, Luo Y. Propagation of new delhi metallo-β-lactamase Genes (blaNDM-1) from a wastewater treatment plant to its receiving river. Environ Sci Technol Lett. 2016;3(4):138-43.
88. O'Toole G, Kaplan HB, Kolter R. Biofilm formation as microbial development. Annu Rev Microbiol. 2000;54(1):49-79.
89. Rosen DA, Hilliard JK, Tiemann KM, Todd EM, Morley SC, Hunstad DA. *Klebsiella pneumoniae* FimK promotes virulence in murine pneumonia. J Infect Dis. 2016;213(4):649-58.
90. McLaughlin MM, Advincula MR, Malczynski M, Barajas G, Qi C, Scheetz MH. Quantifying the clinical virulence of *Klebsiella pneumoniae* producing carbapenemase *Klebsiella pneumoniae* with a *Galleria mellonella* model and a pilot study to translate to patient outcomes. BMC Infect Dis. 2014;14:31.
91. Goris J, Konstantinidis KT, Klappenbach JA, Coenye T, Vandamme P, Tiedje JM. DNA-DNA hybridization values and their relationship to whole-genome sequence similarities. Int J Syst Evol Microbiol. 2007;57:81-91.
92. Delcher AL, Phillippy A, Carlton J, Salzberg SL. Fast algorithms for large-scale genome alignment and comparison. Nucleic Acids Res. 2002;30(11):2478-83.
93. Schwartz S, Kent WJ, Smit A, Zhang Z, Baertsch R, Hardison RC, et al. Human-mouse alignments with BLASTZ. Genome Res. 2003;13(1):103-7.
94. Li H, Durbin R. Fast and accurate short read alignment with Burrows-Wheeler transform. Bioinformatics. 2009;25(14):1754-60.

Tables

Table 1 Genomic mutations of four major classes of virulence factors in NKU_KlebA1 and NKU_Kleb8A7 compare with NKU_Kleb8. NKU_Kleb8 was one pure *K. pneumoniae* strain isolated from SHIME before AMX exposure, NKU_KlebA1 was isolated after AMX exposure, and NKU_Kleb8A7 was evolved from NKU_Kleb8 after AMX exposure.

Vfdb ID	Vfdb Name	Vfdb Function	Function Type	Isolates
VFG000679	*dep/capD*	Gamma-glutamyltranspeptidase, required for polyglutamate anchoring to peptidoglycan	Capsule	NKU_Kleb8A7[b]
VFG000700	*bsc1*	Bifunctional; ribulose 5-phosphate reductase; CDP-ribitol pyrophosphorylase	Capsule	NKU_Kleb8A7[b]
VFG000963	*hasB*	UDP-glucose 6-dehydrogenase	Capsule	NKU_Kleb8A7[b]
VFG001306	*cap8J*	Capsular polysaccharide synthesis enzyme Cap8J	Capsule	NKU_Kleb8A7[b]
VFG001311	*cap8O*	Capsular polysaccharide synthesis enzyme Cap8O	Capsule	NKU_Kleb8A7[b]
VFG001342	*cpsO*	Glycosyl transferase cpso	Capsule	NKU_Kleb8A7[a]
VFG001373	*cps4I*	UDP-N-acetylglucosamine-2-epimerase	Capsule	NKU_Kleb8A7[b]
VFG001964	*Cj1436c*	Aminotransferase	Capsule	NKU_Kleb8A7[b]
VFG001965	*Cj1437c*	Aminotransferase	Capsule	NKU_Kleb8A7[b]
VFG001966	*Cj1438c*	Sugar transferase	Capsule	NKU_Kleb8A7[b]
VFG001971	*kpsF*	D-arabinose 5-phosphate isomerase	Capsule	NKU_Kleb8A7[b]
VFG001988	*cysC*	Adenylylsulfate kinase	Capsule	NKU_Kleb8A7[b]
VFG002182	*cpsI*	UDP-galactopyranose mutase	Capsule	NKU_KlebA1[c]
VFG002189	*cpsB*	Phosphatidate cytidylyltransferase	Capsule	NKU_Kleb8A7[b]
VFG002190	*cpsA*	Undecaprenyl diphosphate synthase	Capsule	NKU_Kleb8A7[b]
VFG002546	*wcbT*	Acyl-coa transferase	Capsule	NKU_Kleb8A7[b]
VFG002548	*wcbR*	Capsular polysaccharide biosynthesis fatty acid synthase	Capsule	NKU_Kleb8A7[b]
VFG002550	*wcbP*	Capsular polysaccharide biosynthesis dehydrogenase/reductase	Capsule	NKU_Kleb8A7[b]
VFG002552	*wcbN*	D-glycero-d-manno-heptose 1,7-bisphosphate phosphatase	Capsule	NKU_Kleb8A7[b]
VFG002563	*wzt2*	ATP-binding ABC transporter capsular polysaccharide export protein	Capsule	NKU_Kleb8A7[b]
VFG002566	*wcbC*	Capsular polysaccharide biosynthesis/export protein	Capsule	NKU_Kleb8A7[b,c]
VFG002567	*wcbB*	Capsular polysaccharide glycosyltransferase biosynthesis protein	Capsule	NKU_Kleb8A7[a]
VFG000113	*pilC*	Still frameshift type 4 fimbrial biogenesis protein pilc	Fimbriae	NKU_Kleb8A7[b]
VFG000114	*xcpA/pilD*	Type 4 prepilin peptidase pild	Fimbriae	NKU_Kleb8A7[b]
VFG000232	*pilT*	Twitching motility protein pilt	Fimbriae	NKU_Kleb8A7[b]
VFG000446	*fimD*	Usher protein fimd	Fimbriae	NKU_KlebA1[a]
VFG000454	*lpfC*	Long polar fimbrial usher protein lpfc	Fimbriae	NKU_KlebA1[c], NKU_Kleb8A7[b]
VFG000455	*lpfB*	Long polar fimbrial chaperone protein lpfb	Fimbriae	NKU_Kleb8A7[b]

Table 1 Genomic mutations of four major classes of virulence factors in NKU_KlebA1 and NKU_Kleb8A7 compare with NKU_Kleb8. NKU_Kleb8 was one pure *K. pneumoniae* strain isolated from SHIME before AMX exposure, NKU_KlebA1 was isolated after AMX exposure, and NKU_Kleb8A7 was evolved from NKU_Kleb8 after AMX exposure (continued).

Vfdb ID	Vfdb Name	Vfdb Function	Function Type	Isolates
VFG000456	*lpfA*	Long polar fimbria protein lpfa	Fimbriae	NKU_Kleb8A7[b]
VFG000871	*fimB*	Type 1 fimbriae Regulatory protein fimb	Fimbriae	NKU_Kleb8A7[b]
VFG000872	*fimE*	Type 1 fimbriae Regulatory protein fime	Fimbriae	NKU_Kleb8A7[b]
VFG000873	*fimA*	Type-1 fimbrial protein, A chain precursor	Fimbriae	NKU_Kleb8A7[b]
VFG000874	*fimI*	Fimbrin-like protein fimi precursor	Fimbriae	NKU_Kleb8A7[b]
VFG000875	*fimC*	Chaperone protein fimc precursor	Fimbriae	NKU_Kleb8A7[b]
VFG000876	*fimD*	Outer membrane usher protein fimd precursor	Fimbriae	NKU_Kleb8A7[b,c]
VFG000877	*fimF*	Fimf protein precursor	Fimbriae	NKU_Kleb8A7[b,c]
VFG000878	*fimG*	Fimg protein precursor	Fimbriae	NKU_Kleb8A7[b]
VFG000879	*fimH*	Fimh protein precursor	Fimbriae	NKU_Kleb8A7[b]
VFG000882	*papA*	P pilus major subunit papa	Fimbriae	NKU_Kleb8A7[a]
VFG000883	*papH*	P pilus termination subunit paph	Fimbriae	NKU_Kleb8A7[a]
VFG000884	*papC*	Usher protein papc	Fimbriae	NKU_Kleb8A7[a]
VFG000885	*papD*	Chaperone protein papd	Fimbriae	NKU_Kleb8A7[a]
VFG000912	*focD*	F1C fimbrial usher	Fimbriae	NKU_KlebA1[c]
VFG001145	*hifB*	Periplasmic chaperone	Fimbriae	NKU_Kleb8A7[b]
VFG001206	*fbpC*	Iron(III ABC transporter, ATP-binding protein	Fimbriae	NKU_Kleb8A7[b]
VFG001213	*pilS*	Two-component sensor pils	Fimbriae	NKU_Kleb8A7[b]
VFG001214	*pilR*	Two-component response regulator pilr	Fimbriae	NKU_Kleb8A7[b]
VFG001225	*pilG*	Twitching motility protein pilg	Fimbriae	NKU_KlebA1[c], NKU_Kleb8A7[b]
VFG001231	*chpA*	Still frameshift probable component of chemotactic signal transduction system	Fimbriae	NKU_KlebA1[a]
VFG001234	*chpD*	Probable transcriptional regulator	Fimbriae	NKU_Kleb8A7[b]
VFG001880	*pilB*	Type IV pilus assembly protein pilb	Fimbriae	NKU_KlebA1[c], NKU_Kleb8A7[b]
VFG002412	*yagY/ecpB*	*E. coli* common pilus chaperone EcpB	Fimbriae	NKU_Kleb8A7[b]
VFG002414	*yagZ/ecpA*	*E. coli* common pilus structural subunit EcpA	Fimbriae	NKU_Kleb8A7[b]
VFG002415	*yagX/ecpC*	*E. coli* common pilus usher EcpC	Fimbriae	NKU_Kleb8A7[b]
VFG002416	*yagW/ecpD*	Polymerized tip adhesin of ECP fibers	Fimbriae	NKU_Kleb8A7[b]

Table 1 Genomic mutations of four major classes of virulence factors in NKU_KlebA1 and NKU_Kleb8A7 compare with NKU_Kleb8. NKU_Kleb8 was one pure *K. pneumoniae* strain isolated from SHIME before AMX exposure, NKU_KlebA1 was isolated after AMX exposure, and NKU_Kleb8A7 was evolved from NKU_Kleb8 after AMX exposure (continued).

Vfdb ID	Vfdb Name	Vfdb Function	Function Type	Isolates
VFG002417	*yagV/ecpE*	*E. coli* common pilus chaperone ecpe	Fimbriae	NKU_Kleb8A7[b]
VFG002428	*pilD*	Type IV prepilin leader peptide type M1	Fimbriae	NKU_Kleb8A7[b]
VFG010463	*pilQ*	Type IV pilus secretin protein pilq	Fimbriae	NKU_Kleb8A7[b]
VFG017856	*pilW*	Type IV fimbrial biogenesis protein pilw	Fimbriae	NKU_Kleb8A7[b,c]
VFG042535	*f17d-A*	F17 fimbrial major subunit protein	Fimbriae	NKU_Kleb8A7[b]
VFG042536	*f17d-D*	F17 fimbrial chaperone	Fimbriae	NKU_Kleb8A7[b]
VFG042537	*f17d-C*	F17 fimbrial uscher	Fimbriae	NKU_Kleb8A7[b]
VFG000033	*bplF*	Lipopolysaccharide biosynthesis protein	LPS	NKU_Kleb8A7[b]
VFG000036	*bplC*	Lipopolysaccharide biosynthesis protein	LPS	NKU_Kleb8A7[b]
VFG000038	*bplA*	Probable oxidoreductase	LPS	NKU_Kleb8A7[b]
VFG000139	*waaG*	B-band O-antigen polymerase	LPS	NKU_Kleb8A7[b]
VFG000142	*waaC*	3-deoxy-D-manno-octulosonic-acid (KDO transferase	LPS	NKU_Kleb8A7[b]
VFG000313	*gluP*	Glucose/galactose transporter	LPS	NKU_Kleb8A7[b]
VFG000320	*kdtB*	Lipopolysaccharide core biosynthesis protein	LPS	NKU_Kleb8A7[b]
VFG000670	*gtrB*	Bactoprenol glucosyl transferase	LPS	NKU_KlebA1[c], NKU_Kleb8A7[b]
VFG002220	*pgm*	Phosphoglucomutase	LPS	NKU_Kleb8A7[b]
VFG002224	*wbkA*	Mannosyltransferase	LPS	NKU_Kleb8A7[a]
VFG002228	*wzt*	O-antigen export system ATP-binding protein	LPS	NKU_Kleb8A7[a]
VFG002230	*wbkC*	GDP-mannose 4,6-dehydratase / GDP-4-amino-4,6-dideoxy-D-mannose formyltransferase	LPS	NKU_Kleb8A7[b]
VFG011453	*wbpZ*	Mannosyltransferase C	LPS	NKU_Kleb8A7[a]
VFG013400	*rfaF*	ADP-heptose-LPS heptosyltransferase II	LPS	NKU_Kleb8A7[b]
VFG000358	*fyuA*	Pesticin/yersiniabactin receptor protein	Siderophores	NKU_Kleb8A7[a]
VFG000359	*ybtE*	Yersiniabactin siderophore biosynthetic protein	Siderophores	NKU_Kleb8A7[b]
VFG000360	*ybtT*	Yersiniabactin biosynthetic protein ybtt	Siderophores	NKU_Kleb8A7[a]
VFG000361	*ybtU*	Yersiniabactin biosynthetic protein ybtu	Siderophores	NKU_Kleb8A7[a]
VFG000362	*irp1*	Yersiniabactin biosynthetic protein Irp1	Siderophores	NKU_Kleb8A7[a]
VFG000363	*irp2*	Yersiniabactin biosynthetic protein Irp2	Siderophores	NKU_Kleb8A7[a]
VFG000364	*ybtA*	Transcriptional regulator ybta	Siderophores	NKU_Kleb8A7[a]

Table 1 Genomic mutations of four major classes of virulence factors in NKU_KlebA1 and NKU_Kleb8A7 compare with NKU_Kleb8. NKU_Kleb8 was one pure *K. pneumoniae* strain isolated from SHIME before AMX exposure, NKU_KlebA1 was isolated after AMX exposure, and NKU_Kleb8A7 was evolved from NKU_Kleb8 after AMX exposure (continued).

Vfdb ID	Vfdb Name	Vfdb Function	Function Type	Isolates
VFG000365	*ybtP*	Lipoprotein inner membrane ABC-transporter	Siderophores	NKU_Kleb8A7[a]
VFG000366	*ybtQ*	Inner membrane ABC-transporter ybtq	Siderophores	NKU_Kleb8A7[b]
VFG000367	*ybtX*	Putative signal transducer	Siderophores	NKU_Kleb8A7[a]
VFG000368	*ybtS*	Salicylate synthase Irp9	Siderophores	NKU_Kleb8A7[b]
VFG000923	*fepA*	Ferrienterobactin outer membrane transporter	Siderophores	NKU_KlebA1[c], NKU_Kleb8A7[b,c]
VFG000924	*fepB*	Ferrienterobactin ABC transporter periplasmic binding protein	Siderophores	NKU_Kleb8A7[b]
VFG000925	*fepC*	Ferrienterobactin ABC transporter atpase	Siderophores	NKU_Kleb8A7[b]
VFG000926	*fepD*	Ferrienterobactin ABC transporter permease	Siderophores	NKU_Kleb8A7[b]
VFG000928	*fepG*	Iron-enterobactin ABC transporter permease	Siderophores	NKU_Kleb8A7[b]
VFG000929	*entD*	Phosphopantetheinyl transferase component of enterobactin synthase multienzyme complex	Siderophores	NKU_KlebA1[c], NKU_Kleb8A7[b]
VFG000930	*entF*	Enterobactin synthase multienzyme complex component, ATP-dependent	Siderophores	NKU_Kleb8A7[b]
VFG000931	*entC*	Isochorismate synthase 1	Siderophores	NKU_Kleb8A7[b]
VFG000932	*entE*	2,3-dihydroxybenzoate-AMP ligase component of enterobactin synthase multienzyme complex	Siderophores	NKU_Kleb8A7[b]
VFG000933	*entB*	Isochorismatase	Siderophores	NKU_Kleb8A7[b]
VFG000934	*entA*	2,3-dihydro-2,3-dihydroxybenzoate dehydrogenase	Siderophores	NKU_Kleb8A7[b,c]
VFG000935	*iroN*	Salmochelin receptor iron	Siderophores	NKU_Kleb8A7[b]
VFG000936	*iutA*	Ferric aerobactin receptor precusor iuta	Siderophores	NKU_KlebA1[c], NKU_Kleb8A7[b]
VFG012501	*iroE*	Esterase	Siderophores	NKU_Kleb8A7[b]
VFG044159	*fes*	Enterobactin/ferric enterobactin esterase	Siderophores	NKU_Kleb8A7[b]
VFG044165	*entS*	Enterobactin exporter, iron-regulated	Siderophores	NKU_Kleb8A7[b]

[a]Emergence of new virulence factor genes not exist in wild type strain NKU_Kleb8;

[b]Appearance of single nucleotide polymorphisms (SNPs) sites compared with_wild type strain NKU_Kleb8;

[c]Appearance of insertion-deletions (InDels) sites compared with_wild type strain NKU_Kleb8

Additional File Legends

Additional file 1: Supplementary information file. **Supplementary Methods. Table S1.** Antibiotic resistance genes (ARGs) related to drug resistance pathways detecting in 8 *Klebsiella* strains from AMX-exposed sample. *bl2b_tem1* and *bl2be_shv2* related to β-lactam resistance; *arna* and *rosb* related to cationic antimicrobial peptide (CAMP) resistance; and *vang* related to vancomycin resistance. **Table S2.** The general feature of the *K. pneumoniae* NKU_KlebA1 genome. **Table S3.** Length and primers of ARGs related to drug resistance pathways detected in *Klebsiella* strains. *bl2b_tem1* and *bl2be_shv2* related to β-lactam resistance; *arna* and *rosb* related to CAMP resistance; and *vang* related to vancomycin resistance. **Fig. S1.** Composition of gut bacterial community at phylum level in three colon regions at different sampling points, in which letters A, T and D mean ascending, transverse, and descending colon, reprehensively. C-A1 and C-A2 represent samples collected from ascending colon at 14 and 21 days

before AMX administration, AMX-A1 and AMX-A2 represent the samples collected from ascending colon at 24 and 28 days during 600 mg/day of AMX treatment, R1-A1 and R-A2 represent the samples collected from ascending colon at 35 and 42 days after termination of AMX. In this way, C-T1, C-T2, AMX-T1, AMX-T2, R-T1, and R-T2 refer the samples from transverse colon at the corresponding days and treatments. C-D1, C-D2, AMX-D1, AMX-D2, R-D1, and R-D2 refer the samples from descending colon at the corresponding days and treatments. **Fig. S2.** Heatmap of the average nucleotide identity (ANI) for strains NKU_KlebA1 and NKU_Kleb8. Colors reflect ANI of two strains from low (red) to high (blue). The area of the ellipse reflect ANI of two strains from low (large) to high (small).

Additional file 2: Excel S1. The mobile elements and metabolic systems of the *K. pneumoniae* NKU_KlebA1.

Additional file 3: Excel S2. Human disease-related systems of the *K. pneumoniae* NKU_KlebA1.

Additional file 4: Excel S3. Genome differences in *Klebsiella* strains.

Figures

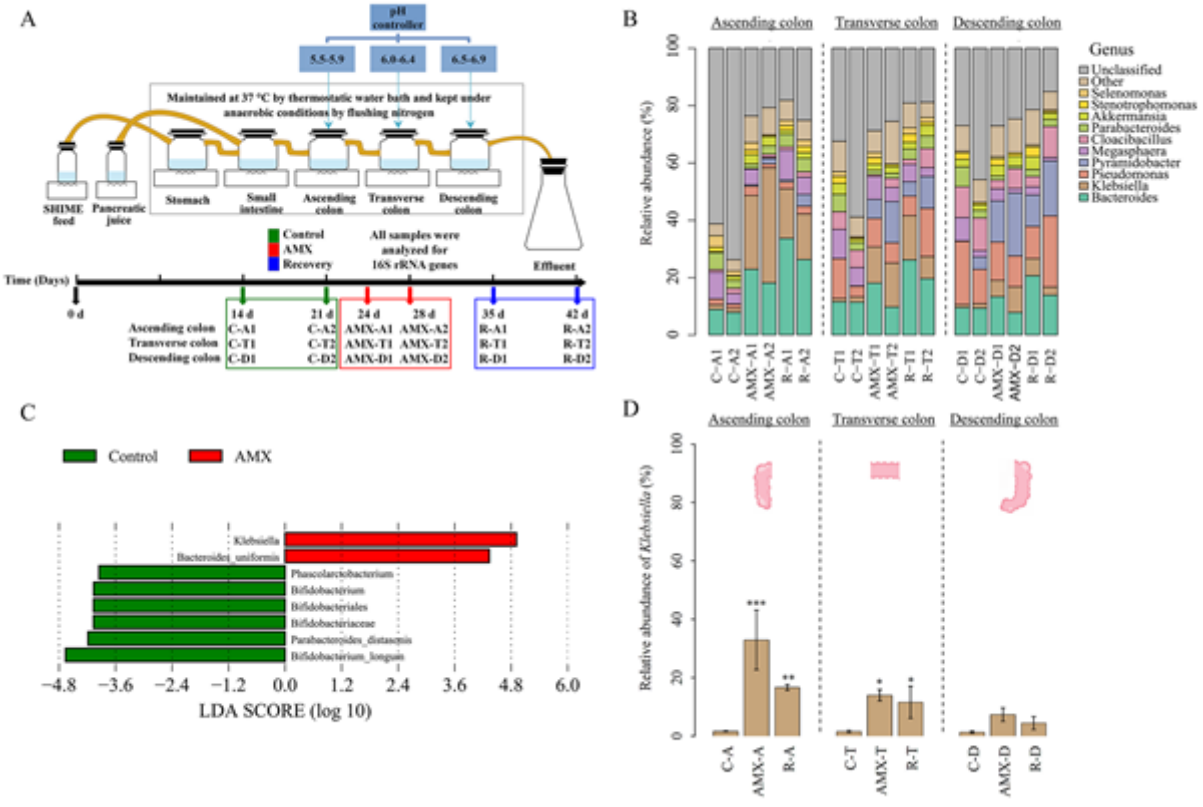

Figure 1

Schematic of designed SHIME model and sampling time point setup (A), in which letters A, T and D mean ascending, transverse, and descending colon, reprehensively. C-A1 and C-A2 represent samples collected from ascending colon at 14 and 21 days before AMX administration, AMX-A1 and AMX-A2 represent the samples collected from ascending colon at 24 and 28 days during 600 mg/day of AMX treatment, R1-A1 and R-A2 represent the samples collected from ascending colon at 35 and 42 days after termination of AMX. In this way, C-T1, C-T2, AMX-T1, AMX-T2, R-T1, and R-T2 refer the samples from transverse colon at the corresponding days and treatments. C-D1, C-D2, AMX-D1, AMX-D2, R-D1, and R-D2 refer the samples from descending colon at the corresponding days and treatments. Composition of gut bacterial community at genus level in three colon regions at different sampling points (B), LEfSe comparison analysis the significant changed bacterial taxa between the AMX-free control and AMX-exposed groups based on an LDA score cutoff of 3.0 and a Mann-Whitney test at a significance level of 0.05 (C), and mean abundance of Klebsiella in the three parts of colon at different treatments (***p < 0.001, **p < 0.01, *p < 0.05; Error bars indicate s.e.) (D).

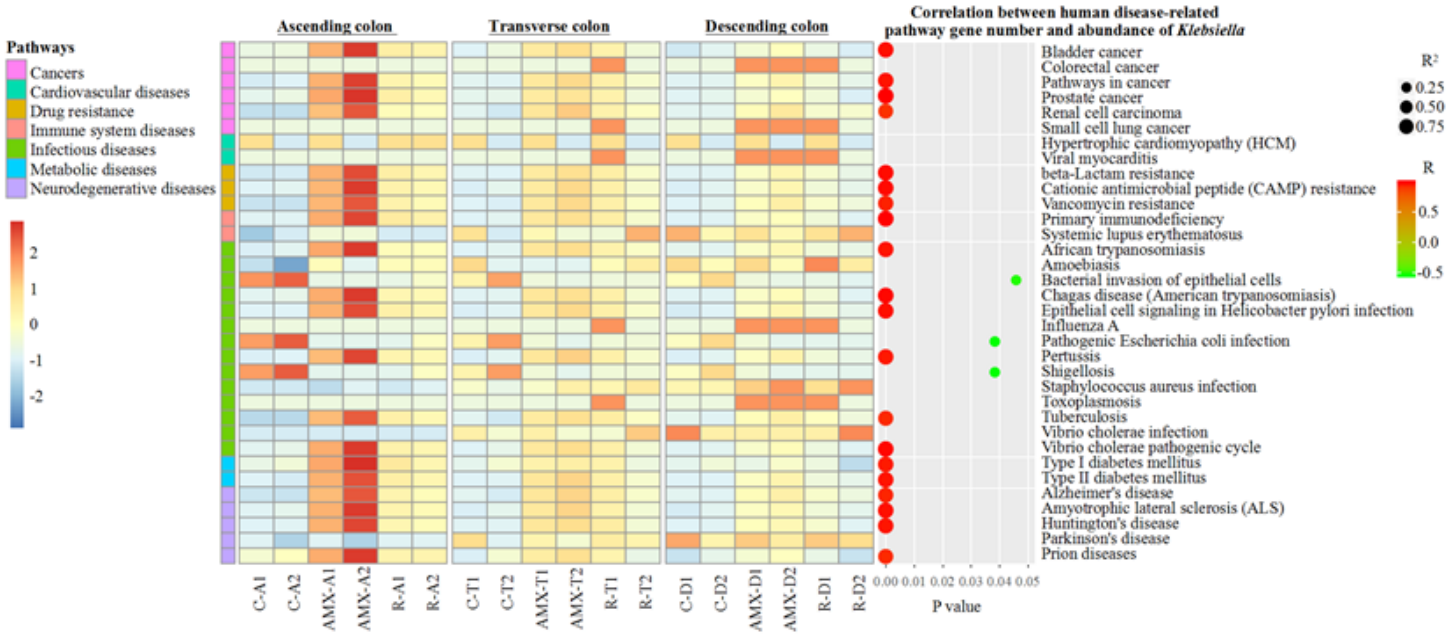

Figure 2

Heatmap of human disease-related pathways in three colon regions at different sampling points and correlation between pathway gene numbers and abundance of Klebsiella. C-A1 and C-A2 represent samples collected from ascending colon at 14 and 21 days before AMX administration, AMX-A1 and AMX-A2 represent the samples collected from ascending colon at 24 and 28 days during 600 mg/day of AMX treatment, R1-A1 and R-A2 represent the samples collected from ascending colon at 35 and 42 days after termination of AMX. In this way, C-T1, C-T2, AMX-T1, AMX-T2, R-T1, and R-T2 refer the samples from transverse colon at the corresponding days and treatments. C-D1, C-D2, AMX-D1, AMX-D2, R-D1, and R-D2 refer the samples from descending colon at the corresponding days and treatments. Colors in heatmap reflect gene numbers level of pathways from low (blue) to high (red). Pearson correlations from negative

(green) to positive (red) between pathway gene numbers and Klebsiella abundances were displayed in the right panel of the figure, and only significant (p value < 0.05) correlations were included.

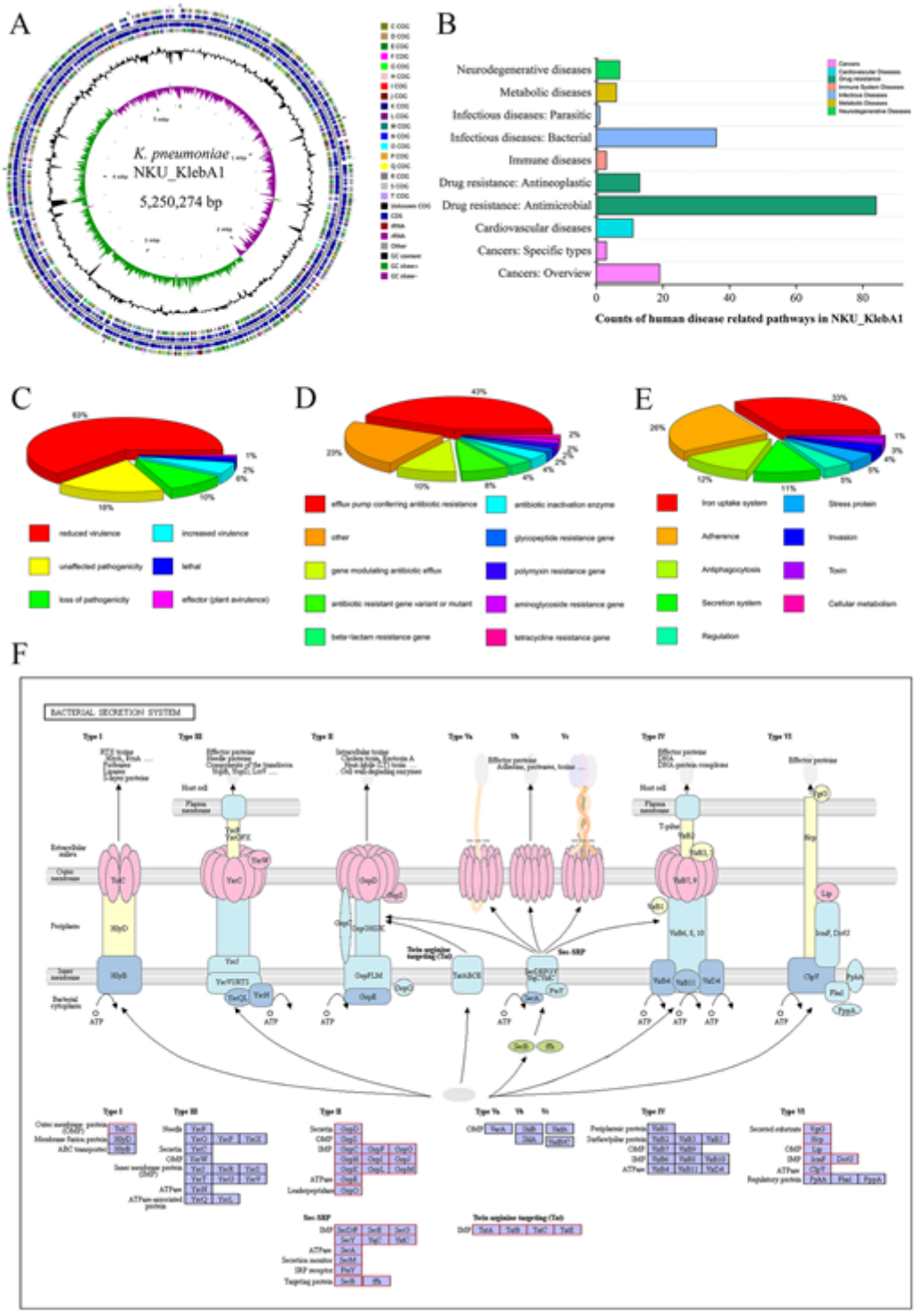

Figure 3

Genomic chromosome maps of the K. pneumoniae NKU_KlebA1 (A), in which from the outside in, the second and third circles show the genes on forward and reverse strands, the first and fourth circles show the predicted protein-encoding regions on the forward and reverse strands, the fifth and sixth circle show

the GC content and GC skew, respectively. KEGG pathways related to human disease annotation (B), human disease-related systems including pathogen-host interactions (C), antibiotic resistance (D), virulence factors (E), and secretion systems (F) of the K. pneumoniae NKU_KlebA1.

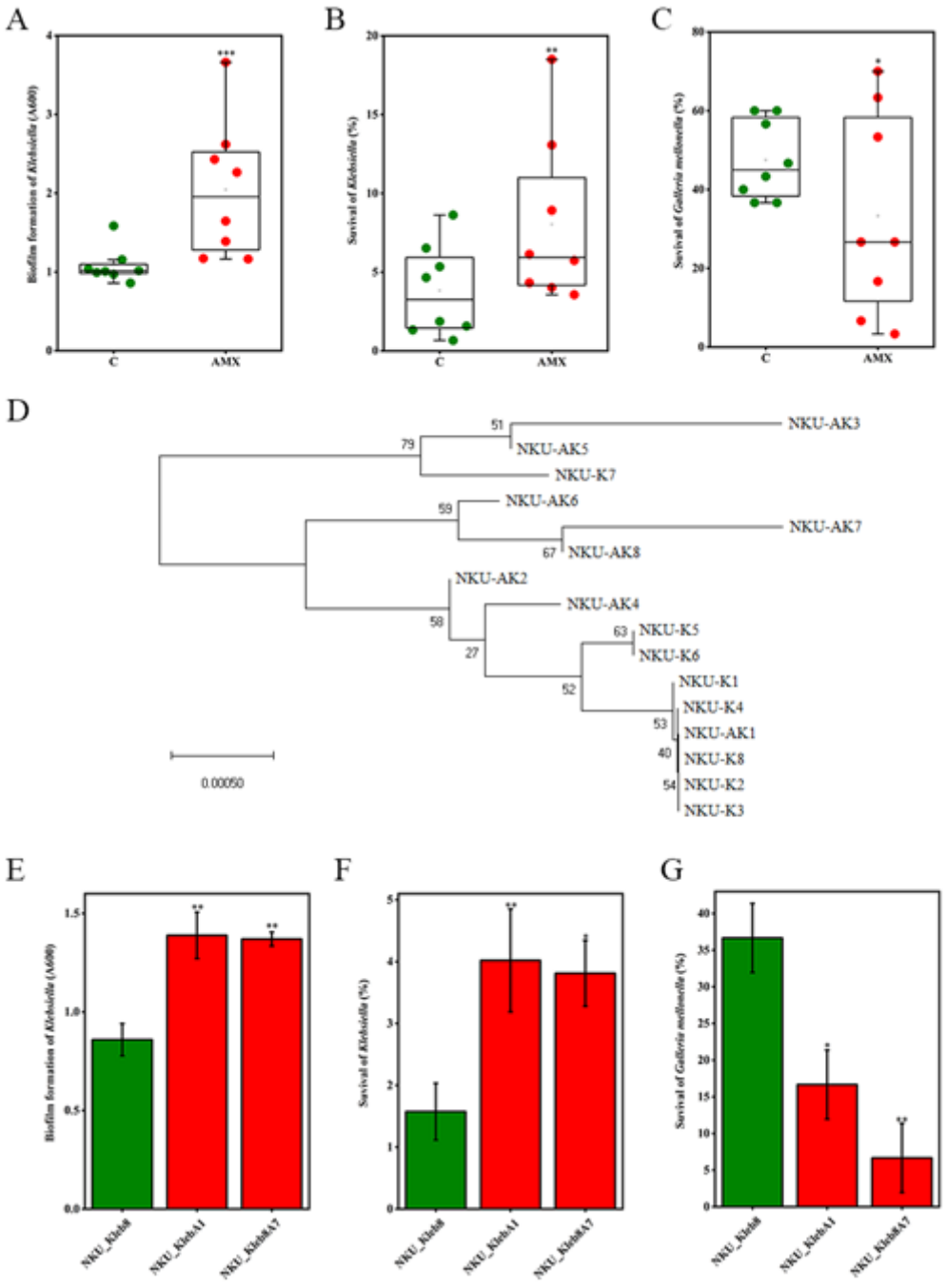

Figure 4

Exposure to AMX promotes biofilm formation (A, E), serum resistance (B, F) and G. mellonella infection capacities (C, G) of isolated K. pneumoniae strains. Comparations between Klebsiella isolates before and after AMX exposure (A-C), in which C represents K. pneumoniae strains isolated before AMX exposure and AMX represents K. pneumoniae strains isolated after AMX exposure (***p < 0.001, **p < 0.01, *p < 0.05; Error bars indicate s.e.). Comparations were also conducted among NKU_Kleb8, NKU_KlebA1 and

NKU_Kleb8A7 (E-G), in which NKU_Kleb8 was isolated before AMX exposure, NKU_KlebA1 and NKU_Kleb8A7 were isolated after AMX exposure (***p < 0.001, **p < 0.01, *p < 0.05; Error bars indicate s.e.). The evolutionary relationships of K. pneumoniae strains (D), in which the sum of branch length = 0.0094 is shown. The percentage of replicate trees in which the associated taxa clustered together in the bootstrap test (1000 replicates) are shown next to the branches.

Supplementary Files

This is a list of supplementary files associated with this preprint. Click to download.

- Additionalfile4.xls
- Additionalfile3.xls
- Additionalfile1.doc
- Additionalfile2.xls